

**The Optical Gravitational Lensing Experiment.  
Gaia South Ecliptic Pole Field as Seen by OGLE-IV\***

I. Soszyński<sup>1</sup>, A. Udalski<sup>1</sup>, R. Poleski<sup>1</sup>, S. Kozłowski<sup>1</sup>,  
Ł. Wyrzykowski<sup>1,2</sup>, P. Pietrukowicz<sup>1</sup>, M.K. Szymański<sup>1</sup>,  
M. Kubiak<sup>1</sup>, G. Pietrzyński<sup>1,3</sup>, K. Ulaczyk<sup>1</sup> and J. Skowron<sup>4,1</sup>

<sup>1</sup>Warsaw University Observatory, Al. Ujazdowskie 4, 00-478 Warszawa, Poland  
e-mail: (soszynsk,udalski,rpoleski,simkoz,wyrzykow,pietruk,msz,mk,pietrzyn,  
kulaczyk,jskowron)@astrouw.edu.pl

<sup>2</sup>Institute of Astronomy, University of Cambridge, Madingley Road, Cambridge  
CB3 0HA, UK

<sup>3</sup>Universidad de Concepción, Departamento de Astronomía, Casilla 160–C, Concepción,  
Chile

<sup>4</sup>Department of Astronomy, Ohio State University, 140 W. 18th Ave., Columbus,  
OH 43210, USA

*Received September 28, 2012*

ABSTRACT

We present a comprehensive analysis of the Gaia South Ecliptic Pole (GSEP) field, 5.3 square degrees area around the South Ecliptic Pole on the outskirts of the LMC, based on the data collected during the fourth phase of the Optical Gravitational Lensing Experiment, OGLE-IV. The GSEP field will be observed during the commissioning phase of the ESA Gaia space mission for testing and calibrating the Gaia instruments.

We provide the photometric maps of the GSEP region containing the mean *VI* photometry of all detected stellar objects and their equatorial coordinates. We show the quality and completeness of the OGLE-IV photometry and color–magnitude diagrams of this region.

We conducted an extensive search for variable stars in the GSEP field leading to the discovery of 6789 variable stars. In this sample we found 132 classical Cepheids, 686 RR Lyr type stars, 2819 long-period, and 1377 eclipsing variables. Several objects deserving special attention were also selected, including a new classical Cepheid in a binary eclipsing system.

To provide empirical data for the Gaia Science Alert system we also conducted a search for optical transients. We discovered two firm type Ia supernovae and nine additional supernova candidates. To facilitate future Gaia supernovae detections we prepared a list of more than 1900 galaxies to redshift about 0.1 located in the GSEP field.

---

\*Based on observations obtained with the 1.3-m Warsaw telescope at the Las Campanas Observatory of the Carnegie Institution for Science.

Finally, we present the results of astrometric study of the GSEP field. With the 26 months time base of the presented here OGLE-IV data, proper motions of stars could be detected with the accuracy reaching 2 mas/yr. Astrometry allowed to distinguish galactic foreground variable stars detected in the GSEP field from LMC objects and to discover about 50 high proper motion stars (proper motion  $\gtrsim 100$  mas/yr). Among them three new nearby white dwarfs were found.

All data presented in this paper are available to the astronomical community from the OGLE Internet archive.

**Key words:** *Techniques: photometric – Astrometry – Catalogs – Stars: variables: general – Stars: oscillations (including pulsations) – binaries: eclipsing – Magellanic Clouds*

## 1. Introduction

The Gaia satellite mission is a flagship scientific mission of the European Space Agency to be launched in the second half of 2013. This is a very ambitious project with the main scientific goal to provide very precise astrometry (accuracy up to 20  $\mu$ as for 15 mag stars), broad band photometry and low resolution spectrophotometry covering wavelength range 300–1000 nm of about 1 billion stars in the Galaxy and Local Group as well as radial velocity measurements of brighter objects from this sample (de Bruijne 2012).

The Gaia hardware will consist of two telescopes with an aperture of  $1.45 \times 0.5$  m each imaging the sky on the focal plane where the main scientific instrument consisting of 106 thin CCDs, in total almost 1 billion pixels, is located. The focal plane CCDs will be divided to sky mapping, astrometric, blue and red spectrophotometric and radial velocity arrays. The satellite is supposed to work in continuous sky scanning mode, so the images will drift continuously through the subsequent arrays filling the entire focal plane where the appropriate measurements will be carried out. The satellite will be placed on the orbit around the Sun-Earth L2 Lagrange point, about 1.5 million km from the Earth. The mission duration is supposed to be at least five years.

After launching, during the commissioning phase, the Gaia satellite will be operated in the scanning mode different from the nominal one to observe more frequently some regions of the sky for calibration purposes and testing the performance of instrumentation. It will cover the ecliptic poles collecting data with higher than typical cadence. One of these regions, namely located close to the southern ecliptic pole, falls on the outskirts of the Large Magellanic Cloud – the sky area monitored regularly by the Optical Gravitational Lensing Experiment in its fourth phase OGLE-IV. Throughout this paper we will call this region of the LMC as the Gaia South Ecliptic Pole field (GSEP).

The GSEP field consists of four OGLE-IV pointings and has been monitored regularly in the standard *VI* bands since 2010. Since then the number of epochs collected in the *I*-band reached several hundreds. Several tens of *V*-band observations were also secured for color information. This dataset is large enough to perform complete analysis of the field as seen from the ground and to provide its full characterization. For example, it is possible to conduct very extensive and effective

search for variable stars, optical transients and analysis of stellar populations. The long time span of observations also allows the determination of precise astrometry of the field. In all these applications the Gaia satellite is supposed to bring new and more precise space measurements, so the direct comparison with the most precise ground base data will be crucial for evaluation of the actual performance of the satellite.

The OGLE photometry is regarded as one of the most precise available from the ground. Moreover, the first results from the OGLE-IV phase indicate that it outperforms that collected in the previous phases. The OGLE-IV photometry of the GSEP field may be, then, an ideal observational material for the Gaia mission for comparison and tests when launched. Therefore we decided to analyze and make the data of the GSEP region of the LMC available well ahead the entire OGLE-IV LMC data are released.

In the past, part of the GSEP region of the LMC was also observed from the ground by the EROS microlensing survey (Tisserand *et al.* 2007) in the years 1996–2003. Additionally, the VISTA VMC Survey (Cioni *et al.* 2011) covered the GSEP field in the near-infrared. However, these data can only be complementary to the optical photometry by providing infrared colors. The number of collected epochs is inadequate for more advanced applications as, for example, a search for variable or transient objects.

Here we present a comprehensive analysis of the OGLE-IV data of the GSEP region in the LMC. First, we show the quality of data, completeness of the OGLE-IV photometry of this region of the LMC and color–magnitude diagrams of the GSEP sub-fields. Then, we present the results of an extensive search for variable stars conducted in the GSEP field detecting 6789 variable objects down to  $I \approx 21$  mag. Among them 132 are classified as classical Cepheids, 686 as RR Lyr type stars, 2819 as long-period and 1377 as eclipsing variables. We also searched for transient objects detecting two firm supernovae and nine supernova candidates in the background galaxies. For facilitating future detections of supernovae we prepared a list of galaxies seen in the GSEP field. Finally, we present proper motions of stars from the GSEP field which with the time baseline of the OGLE-IV observations reach the precision better than 2 mas/yr. Astrometry allowed to distinguish foreground galactic objects from genuine LMC stars. Also a few high proper motion stars and nearby foreground white dwarfs were found. The accuracy of astrometry should improve with time and at the time of the Gaia operation should reach 1 mas/yr.

All the OGLE-IV data presented here are available to the astronomical community from the OGLE Internet archive.

## 2. Observational Data

The OGLE-IV survey is conducted with the 1.3-m Warsaw telescope at the Las Campanas Observatory in Chile. The observatory is operated by the Carnegie Institution for Science. During the OGLE-IV phase the Warsaw telescope is equipped

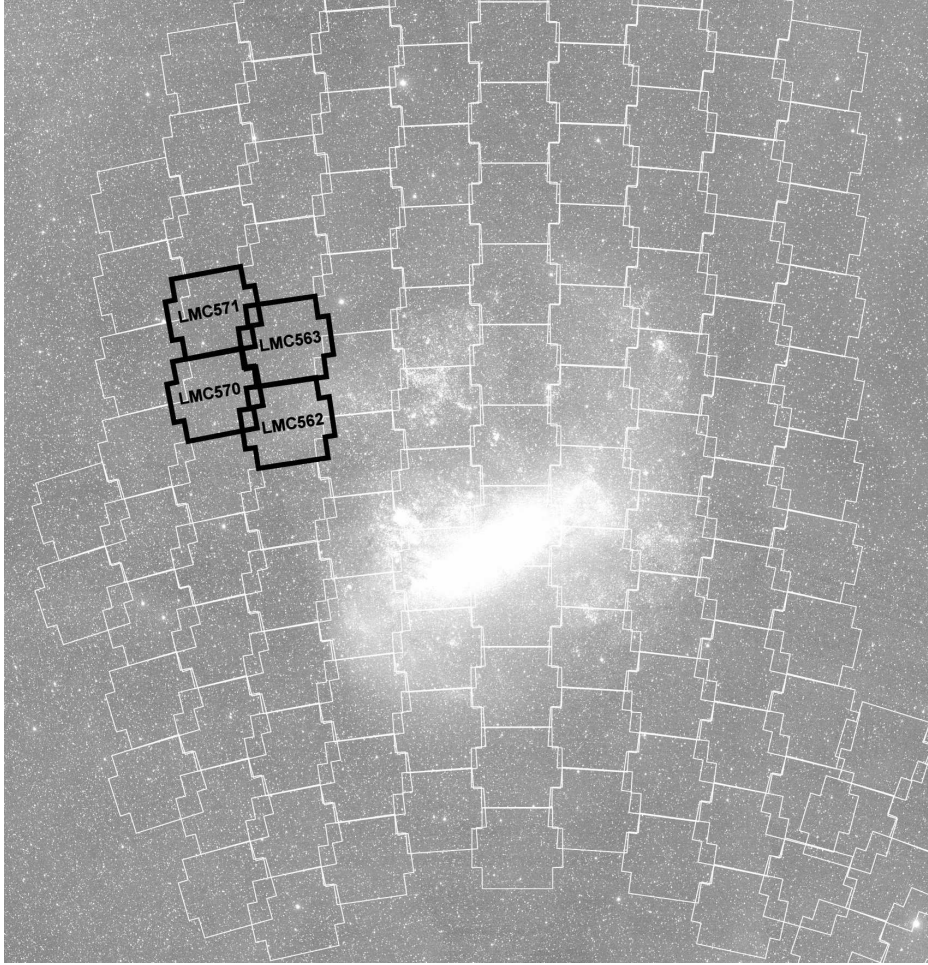


Fig. 1. Gaia South Ecliptic Pole field in the LMC (black contours). White contours show other OGLE-IV fields in the LMC. The background image of the LMC was taken by the ASAS wide field sky survey (Pojmański 1997).

with the “third generation” mosaic camera with 32 thin E2V44-82  $2048 \times 4102$  pixel CCD detectors. The new camera covers approximately 1.4 square degrees on the sky with the scale of 0.26 arcsec/pixel. Detailed description of the OGLE-IV instrumentation can be found at the OGLE WWW site:

*<http://ogle.astrouw.edu.pl/main/OGLEIV/mosaic.html>*

The GSEP field consists of four OGLE-IV pointings with the standard OGLE-IV designations: LMC562, LMC563, LMC570 and LMC571. Due to high southern declination of the LMC fields and the constraints resulting from the sky mosaicing pattern and the shape of the camera field of view, the individual fields overlap quite significantly in some parts. Fig. 1 presents the location of the GSEP field in the LMC. Table 1 lists the equatorial coordinates of the centers of the four GSEP

subfields. They cover an area of about 5.3 square degrees. The total number of stars detected in the *I*-band exceeds 1.6 million – the appropriate numbers for each subfield are also listed in Table 1.

T a b l e 1  
OGLE-IV pointings in the GSEP Field

Field	RA (2000)	DEC (2000)	$N_{\text{Stars}}$
LMC562	5 <sup>h</sup> 55 <sup>m</sup> 28 <sup>s</sup>	−67°27′45″	605 304
LMC563	5 <sup>h</sup> 53 <sup>m</sup> 47 <sup>s</sup>	−66°13′55″	445 912
LMC570	6 <sup>h</sup> 05 <sup>m</sup> 56 <sup>s</sup>	−66°50′50″	342 033
LMC571	6 <sup>h</sup> 03 <sup>m</sup> 51 <sup>s</sup>	−65°37′00″	272 300

The GSEP subfields were photometrically monitored from March 6, 2010. The last observations used in this analysis were collected on June 6, 2012. During that time we secured between 338 and 351 data points in the Cousins *I*-band and 29 points in the *V*-band. The exposure time was 150 seconds for both *V*- and *I*-band observations.

Photometry was obtained using the OGLE-IV photometric pipeline designed for real time data reduction at the telescope. It is based on the OGLE-III data pipeline (Udalski 2003) and the photometry is derived with the Difference Image Analysis (DIA) technique (Alard and Lupton 1998, Woźniak 2000).

The *I*-band magnitudes of stars measured by OGLE range from 13 mag to 21 mag. The basic astrometric transformations between the pixel grid and equatorial coordinates were based on the 2MASS Catalog coordinate grid as in the case of the OGLE-III photometric maps (Szymański *et al.* 2011).

### 3. OGLE-IV Photometry of the Gaia South Ecliptic Pole Field

The GSEP field is located on the outskirts of the LMC and belongs to relatively empty fields. Photometry of stellar objects detected on the *I*-band reference images was stored in the individual databases for each of the OGLE-IV GSEP subfields and CCD detectors (*e.g.*, lmc562.01, ..., lmc562.32). Instrumental photometry was calibrated to the standard *VI* system in two steps. First, we used the OGLE-III LMC Photometric Maps (Udalski *et al.* 2008) as a huge list of secondary standards. Comparison of the OGLE-IV photometry of the fields fully overlapping with the OGLE-III maps collected on several photometric nights allowed to derive color-term of OGLE-IV filters, large scale photometry correction resulting among other factors from the change of the scale in the large field of view of the OGLE camera, and the photometry zero point. Only bright and non-variable stars were selected for this comparison. This step required, of course, prior conversion of the OGLE-IV database photometry to the aperture photometry scale by the determination of appropriate aperture corrections.

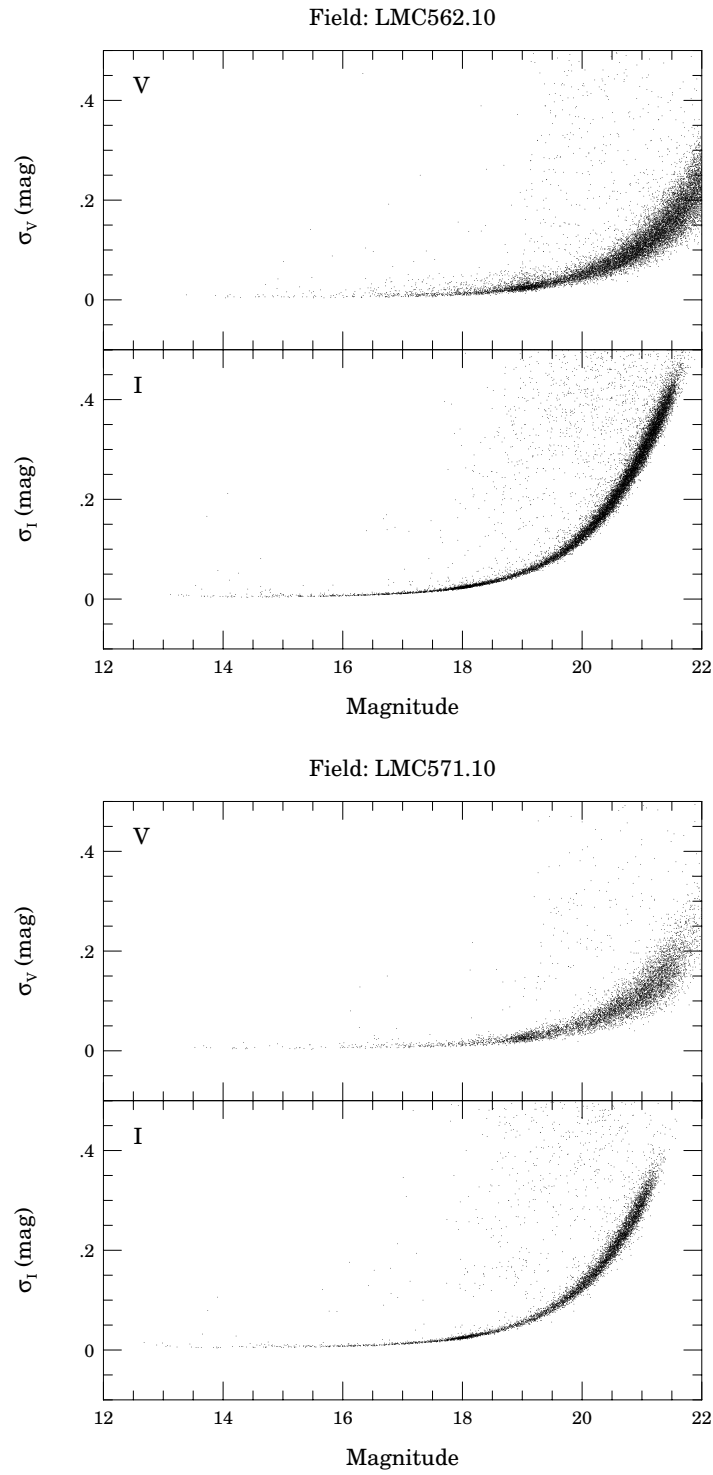


Fig. 2. Standard deviation of magnitudes as a function of magnitude for the subfields LMC562.10 (denser region in the GSEP field) and LMC571.10 (more sparse region).

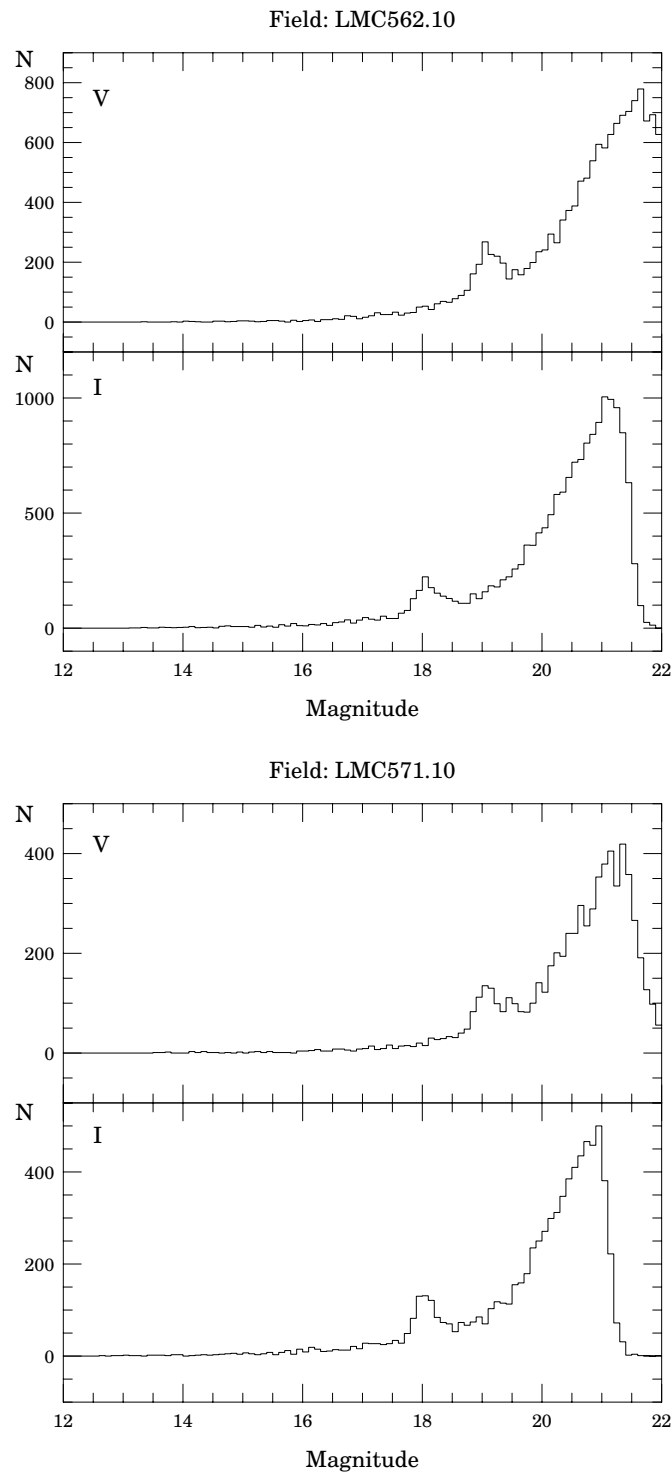


Fig. 3. Histograms of star counts as a function of magnitude in the subfields LMC562.10 and LMC571.10.

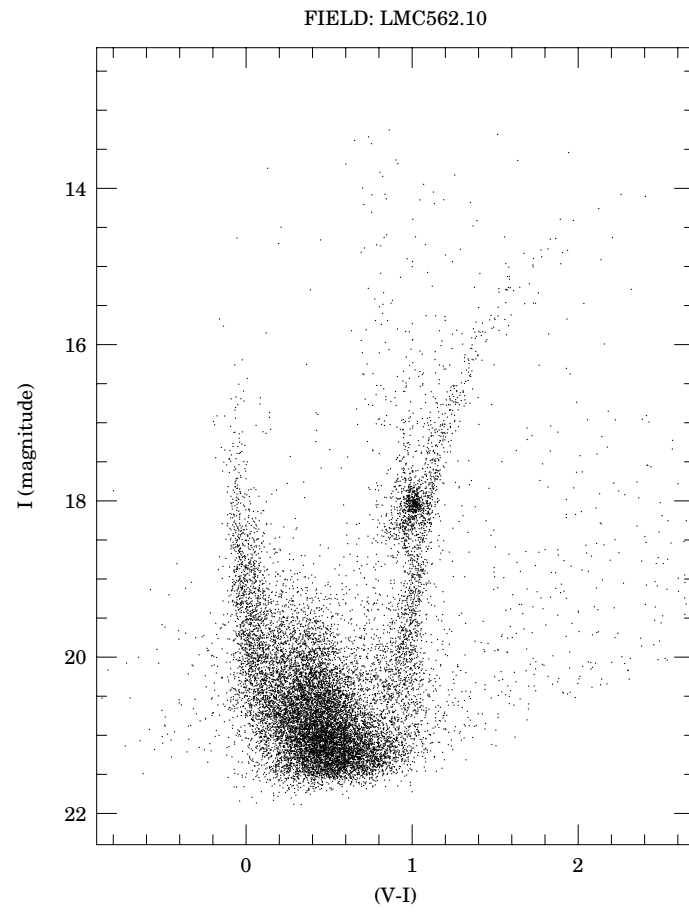


Fig. 4. Color-magnitude diagram of the subfield LMC562.10.

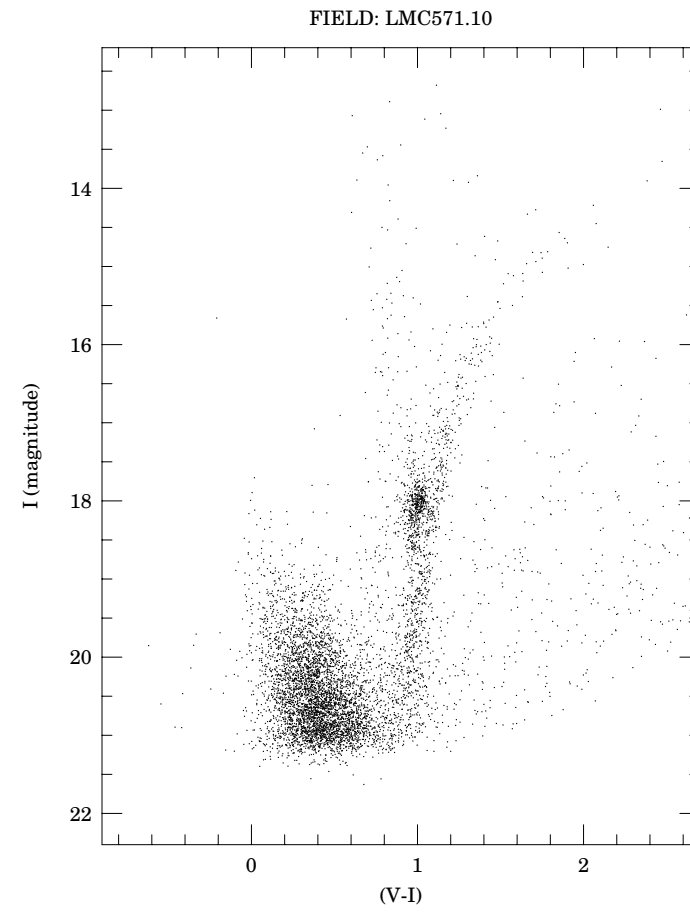


Fig. 5. Color-magnitude diagram of the subfield LMC571.10.



Having the transformation parameters from the comparison of the OGLE-IV photometry with photometric standards (OGLE-III maps) derived in the previous step, the appropriate transformations to the photometry of the GSEP images were applied for each photometric night. The final calibration of the instrumental GSEP databases was the average of individual calibrations from these nights. We estimate the accuracy of zero points of the final photometry to be about 0.03 mag.

Average *VI* photometry of all objects detected in the *I*-band reference images combined with the derived equatorial coordinates, namely the OGLE-IV photometric maps of the GSEP field, were prepared in the same manner as for the OGLE-III maps (Szymański *et al.* 2011). The maps provide information for fast assessment of the quality of the OGLE-IV photometry. Fig. 2 shows the standard deviation as a function of magnitude for typical subfields LMC562.10 (denser region of the GSEP field) and LMC571.10 (sparse stellar density) for *V*- and *I*-band. As one can see the OGLE-IV accuracy of photometry falls to 0.1 mag at  $V \approx 21$  mag and  $I \approx 20$  mag which is roughly comparable with the Gaia expected performance.

Fig. 3 presents histograms of the number of detected stars as a function of magnitude in 0.1 mag bins for the same subfields. The OGLE-IV photometry is complete to about 21.5 mag and 21.0 mag in the *V*- and *I*-band, respectively.

Figs. 4 and 5 present color–magnitude diagrams of the LMC562.10 and LMC571.10 subfields. Both show typical features of the CMDs from the LMC fields (*cf.* Udalski *et al.* 2008) including the main sequence stars strip, red giant branch, and prominent red clump.

Large number of good resolution images collected during the OGLE-IV survey allows construction of much deeper color–magnitude diagrams by stacking such high quality images. Although not done yet, it is planned to make deep OGLE maps of the all observed fields in the Magellanic Clouds.

#### 4. Search for Variable Stars

Search for variable objects in the GSEP field began with the period search conducted on the *I*-band light curves of all detected stars. We used the FNPEAKS program (Z. Kołaczowski, private communication) which analyzes the Fourier spectra of the light curves. The search was performed in the frequency range  $0 - 24 \text{ day}^{-1}$ , with the resolution of  $5 \times 10^{-5} \text{ day}^{-1}$ . To avoid daily aliases the period search for long-period variables was limited to the maximum frequency of  $0.5 \text{ day}^{-1}$ .

The selection and classification of variable stars was based primarily on the light curve shapes. We visually inspected all *I*-band light curves brighter than  $I = 17$  mag. For fainter stars we examined the light curves with signal to noise of the most prominent peak in the periodogram larger than 4.5. Our final classification took into account the morphology of the light curves, mean *I*-band magnitudes,  $(V - I)$  colors, near-infrared *JHK* magnitudes from the 2MASS Point-Source Cat-

alog (Cutri *et al.* 2003) and ratios of periods (for multi-periodic stars). In total we visually examined 135 172 light curves, finding 6789 variable stars.

#### 4.1. *Catalog of Variable Stars in the GSEP Field*

All stars detected in the GSEP field of the LMC and classified as variables are listed in the Catalog of Variable Stars in the GSEP Field which is described below. It is supposed to be a part of the main OGLE Catalog of Variable Stars which will be published in the future, when OGLE-IV data will be gradually released. It is provided in the electronic form in the OGLE Internet archive (see Section 7) and as such it is expected to be updated when more data are available, more precise calibrations are derived, and some unavoidable errors are noticed and corrected.

The list of all variable stars is given in the file `list.dat`. This file contains a table with the following columns: star ID (LMC`NNN.MM.KKK`, where `NNN` is the field number, `MM` indicates the CCD chip number of the mosaic camera, and `KKK` is the star number in the OGLE-IV database), J2000 equatorial coordinates, type of variability, subtype or secondary type of variability, mean *I*- and *V*-band magnitudes, period for periodic stars – derived with the TATRY code kindly provided by Schwarzenberg-Czerny (1996), peak-to-peak *I*-band amplitude, and the secondary period for double- and multi-periodic stars. Cross-identifications with the General Catalogue of Variable Stars (GCVS) and remarks on interesting objects are given in the file `remarks.dat`.

The time-series *I*- and *V*-band photometry of the stars is stored in the directory `phot/`. Finding charts for all stars can be downloaded from the directory `fcharts/`. These are  $60'' \times 60''$  subframes of the *I*-band DIA reference images. See the README file for more details. Figs. 6 and 7 present examples of the periodic and non-periodic light curves of variable stars from the GSEP field catalog.

#### 4.2. *Completeness of the Catalog*

The completeness of our catalog of the GSEP field was assessed by checking our efficiency of the variable star selection in the overlapping parts of adjacent fields. Assuming that the minimum number of observing points must be larger than 50, in total 378 variable stars from our catalog were recorded in the OGLE-IV databases twice – in the neighboring fields, so we had an opportunity to independently detect 756 counterparts. As a result of our variability search we found 646 of them, which yields the completeness of our search method of 83%. The completeness of the whole catalog depends additionally on the efficiency of the star detection in the OGLE fields, which strongly depends on their brightness. The completeness for stars fainter than  $I = 21$  mag drops rapidly (see Section 3).

The verification of the missing 110 counterparts showed that they are almost exclusively very faint or very low-amplitude stars, close to the detection limits of the OGLE-IV survey. Light curves of the faintest stars (with  $I > 20$  mag) are affected by large scatter, which lowers the signal-to-noise ratios of their periodicities

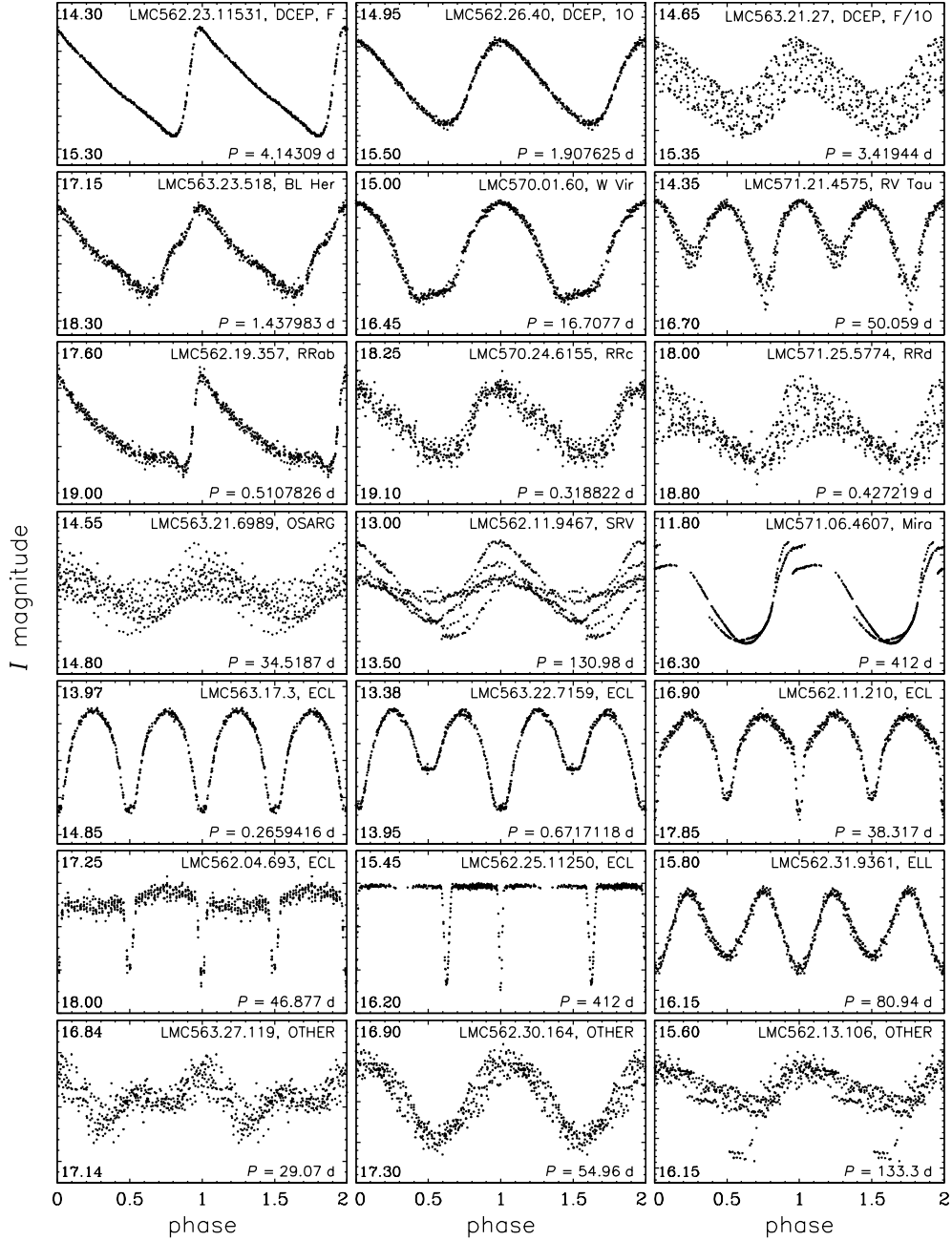


Fig. 6. Examples of the  $I$ -band light curves of periodic variable stars from the GSEP field. Successive rows show the following types of variability: classical Cepheids, type II Cepheids, RR Lyr stars, long-period variables, eclipsing and ellipsoidal binary systems and other variables. Note that the range of magnitudes varies from panel to panel. Numbers in the left corners show the minimum and maximum magnitudes of the range.

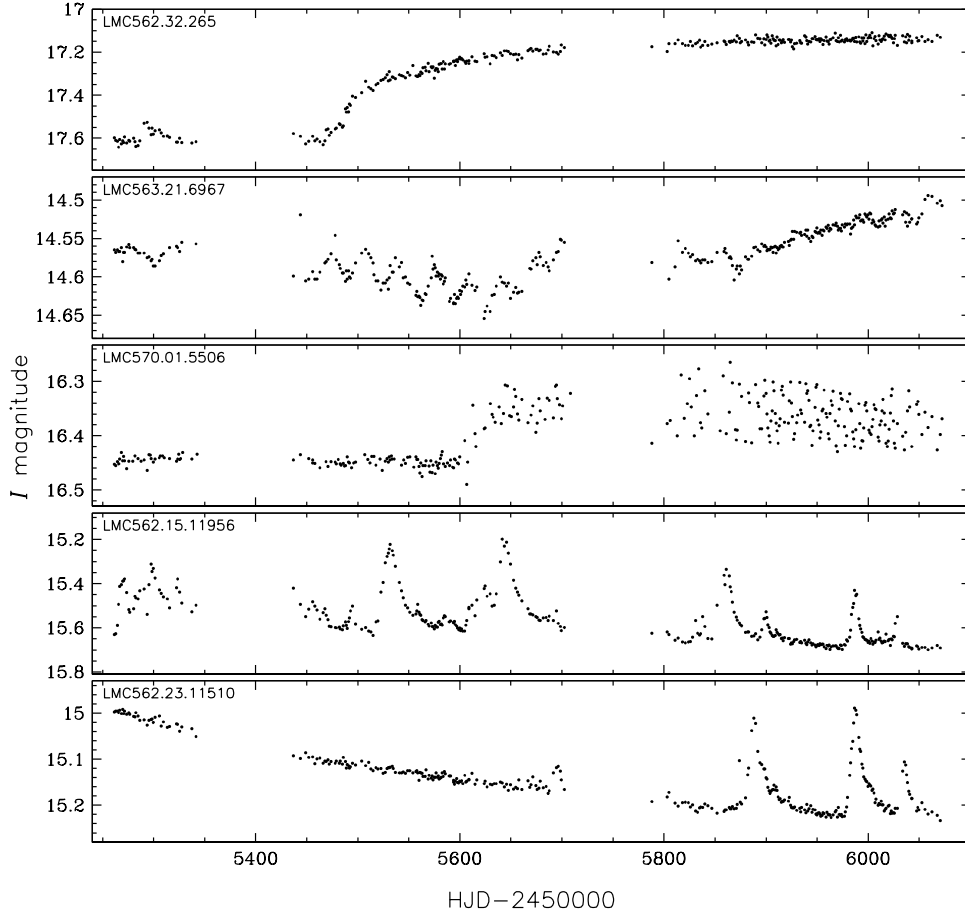


Fig. 7. Examples of the *I*-band light curves of non-periodic variables from the Catalog of Variable Stars in the GSEP Field.

below the detection thresholds applied in this study. The very low-amplitude stars were usually missed during the visual examination. OGLE small amplitude red giants, faint eclipsing binaries and  $\delta$  Sct stars dominate in the group of missed objects. We found all counterparts for Cepheids, RR Lyr stars, semiregular variables and Miras.

We also searched the GCVS Vol.V. Extragalactic Variable Stars (Artyukhina *et al.* 1995) for previously known variable stars in the region covered by our catalog. A total number of 70 variables was found in the GCVS, of which 48 objects were independently identified in our analysis. A careful inspection of the missed 22 stars showed that: eight objects are too bright and saturate in the OGLE frames, seven stars fell into the gaps between the CCD chips of the OGLE-IV mosaic camera, for five objects we cannot confirm their variability (OGLE photometry shows non-variable stars within errors), and two objects exhibit low-amplitude variations, close to our detection limits. These two stars were added to the present catalog and

classified as OTHER variables. The comparison to the GCVS confirms that the completeness of our catalog is high, with the exception of faint or low-amplitude stars.

#### 4.3. *OGLE-IV Variable Stars in the GSEP Field*

Table 2 lists the numbers of variable stars of different types included in the catalog. In some cases our classification is not unique, since some stars exhibit two types of variations, usually originated from pulsations and binarity. For example our catalog contains a classical Cepheid showing eclipses or ellipsoidal variables exhibiting OGLE Small Amplitude Red Giant (OSARG) oscillations.

Table 2

Number of variable stars of different variability types

Variability type	Flag	Number of stars
classical Cepheids	DCEP	132
type II Cepheids	T2CEP	5
anomalous Cepheids	ACEP	3
RR Lyr stars	RRLYR	686
$\delta$ Sct stars	DSCT	159
long-period variables	LPV	2819
eclipsing binaries	ECL	1377
ellipsoidal variables	ELL	156
other variables	OTHER	1473

Below we present a short summary of the content of our GSEP Field Catalog regarding different types of stellar variability.

#### *Classical Cepheids*

Most of the variable stars known to date in the region covered by this study are classical Cepheids. The majority of them were discovered by the Harvard survey for variable stars in the Magellanic Clouds (Leavitt 1908, Shapley and Mohr 1933, Wetzel 1955). Our catalog contains 132 classical Cepheids, 38 of them were included in the GCVS (five with wrong classification). Fifty seven of our Cepheids pulsate solely in the fundamental mode (F), sixty are single-mode first-overtone pulsators (1O), one object is a single-mode second-overtone Cepheid (2O). Four stars are double-mode F/1O Cepheids and ten objects pulsate simultaneously in the first two overtones (1O/2O). Fig. 8 shows the spatial distribution of classical Cepheids in the four OGLE-IV fields. Note the sharp edge of the fundamental-mode Cepheid distribution crossing the LMC562 field. This reflects the distribution of the young stellar population in the LMC, seen also in the CMDs (Figs. 4 and 5). The overtone and double-mode Cepheids are distributed more homogeneously over

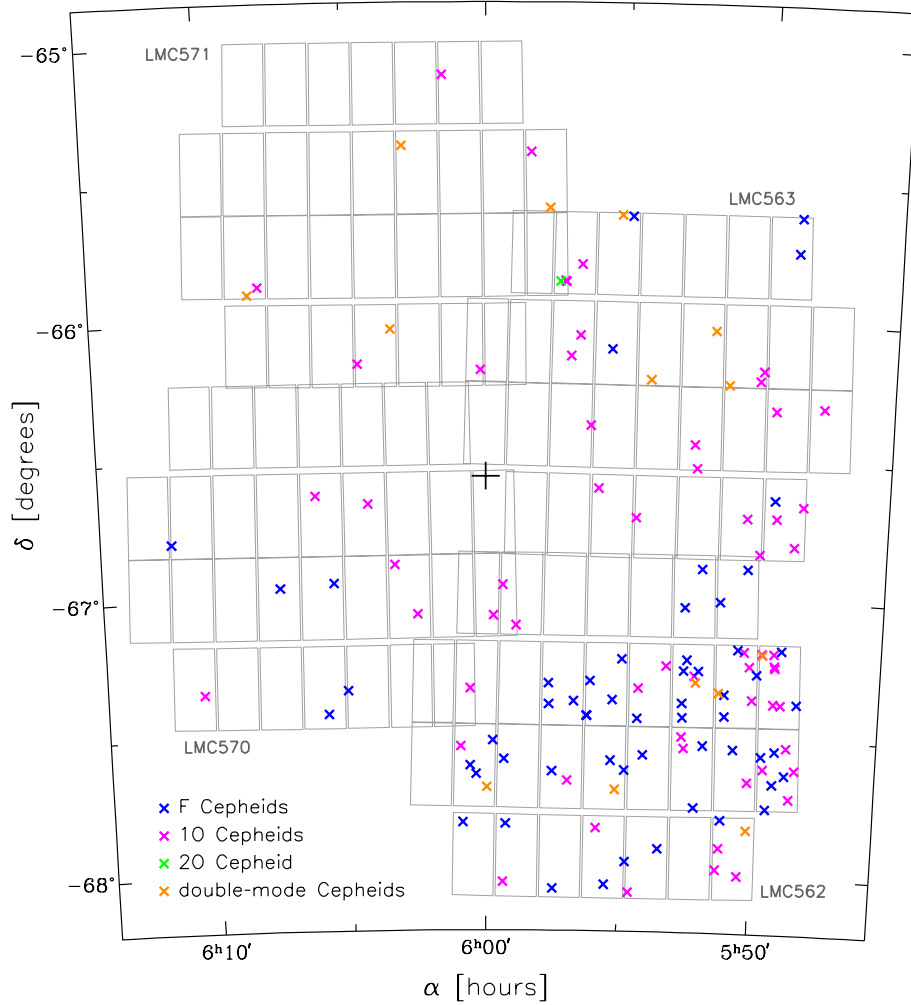


Fig. 8. Spatial distribution of classical Cepheids in the GSEP field. Gray contours show the sky coverage by the individual chips of the OGLE-IV mosaic CCD camera. Blue, magenta, green and orange symbols represent fundamental-mode, first-overtone, second-overtone and double-mode pulsators, respectively. Black cross indicates the position of the South Ecliptic Pole.

the studied area. The positions of double-mode Cepheids, RR Lyr stars and  $\delta$  Sct stars in the Petersen diagram (*i.e.*, the plot of period-ratio against the logarithm of the longer period) is shown in Fig. 9.

We should stress here that an object designated as LMC562.05.9009 is worth of particular interest. It belongs to a rare class of classical Cepheids in eclipsing binary systems. Another Cepheid in the LMC (OGLE-LMC-CEP-0227) which is a member of an eclipsing binary system was recently used for the first determination of the dynamical Cepheid mass with the 1% accuracy (Pietrzyński *et al.* 2010). OGLE-LMC-CEP-1812 system is another example of such very rare systems (Pietrzyński *et al.* 2011).

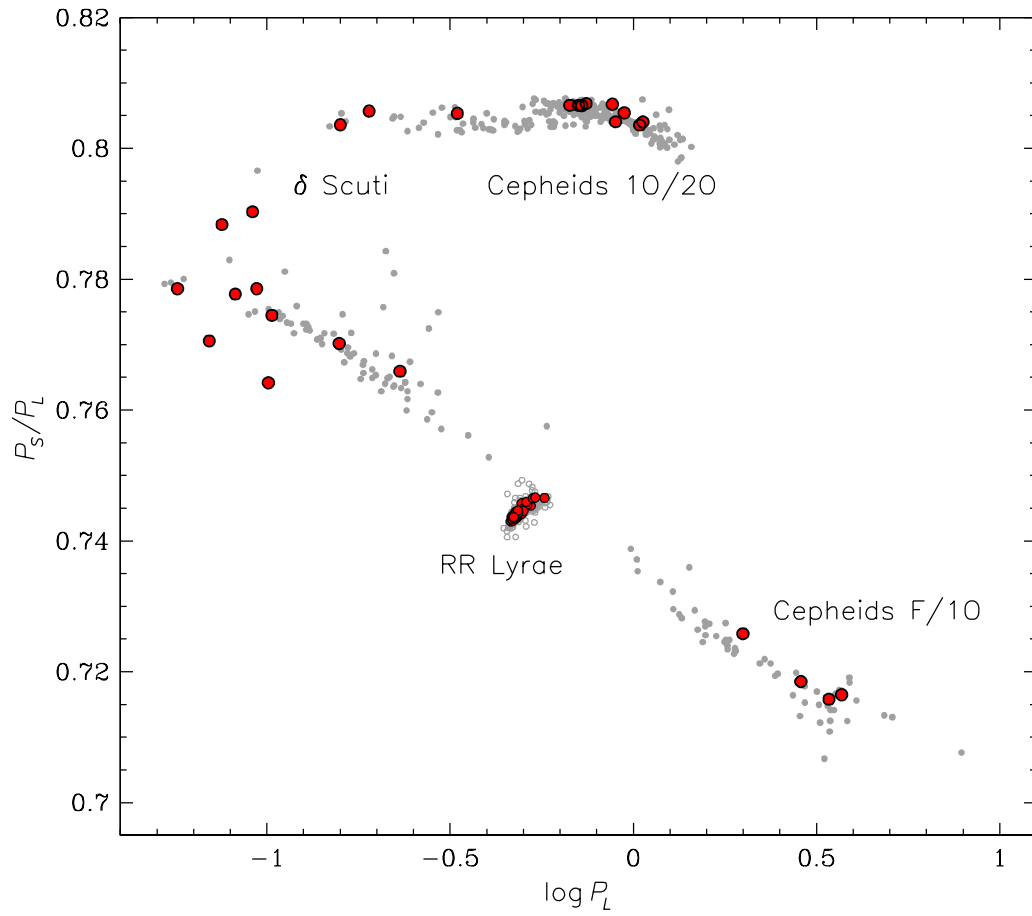


Fig. 9. Petersen diagram for double-mode classical Cepheids, RR Lyr stars and  $\delta$  Sct variables. Red symbols show objects in the GSEP field, while gray points indicate LMC variables from the OGLE-III Catalog of Variable Stars (Soszyński *et al.* 2008, 2009a, Poleski *et al.* 2010a).

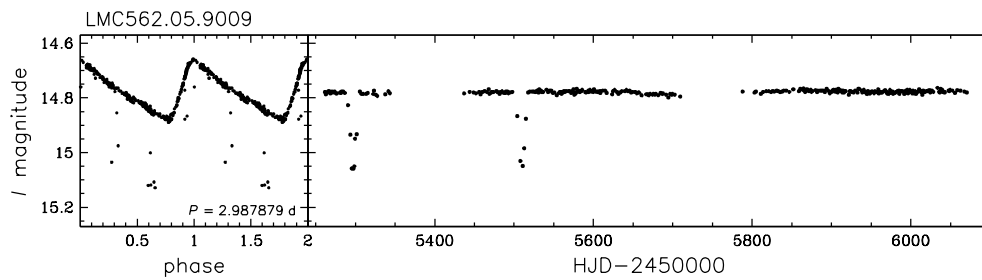


Fig. 10. Light curve of a classical Cepheid LMC562.05.9009 exhibiting eclipsing variations. *Left panel* shows the original photometric data folded with the pulsation period. *Right panel* shows the unfolded light curve after subtracting the Cepheid component.

The light curve of LMC562.05.9009 is presented in Fig. 10. So far, the OGLE observations covered only two eclipses during the seasons 2009/2010 and 2010/2011, and currently it is impossible to determine the orbital period of the system. The lack of eclipses during the 2011/2012 season suggests an eccentric orbit. The system has already been extensively followed-up both photometrically and spectroscopically.

#### *Type II and Anomalous Cepheids*

The OGLE Catalog of the GSEP field contains five stars classified as type II Cepheids (one was already known). This sample consists of one BL Her star, one W Vir star, two RV Tau stars, and one yellow semiregular variable (SRd). There are three anomalous Cepheids in our catalog (two fundamental-mode and one first-overtone pulsator) and all of them are new findings. The classification of LMC563.31.241 is uncertain, since it has a short period (0.5575 days) – typical for RR Lyr stars. However, this object is more luminous than a typical RR Lyr star from the LMC, and its light curve morphology resembles that of the fundamental-mode anomalous Cepheids.

#### *RR Lyr and $\delta$ Sct Stars*

RR Lyr stars are well known tracers of the old stellar population. The OGLE-III catalog of RR Lyr stars in the LMC (Soszyński *et al.* 2009a) contains the largest collection of these stars (24 906) found in any stellar environment. The present sample contains 686 RR Lyr stars, nine of which belong to the Milky Way and the remaining stars being members of the LMC. Two Galactic RR Lyr stars from this sample are present in the GCVS. Our catalog contains 482, 164 and 40 RRab, RRC and RRD stars, respectively. Hypothetical second-overtone pulsators (RRe stars) were not distinguished from the RRC stars. The homogeneous spatial distribution of RR Lyr stars in our fields (Fig. 11) reflects the widely extended halo of the old stellar population in the LMC.

The catalog of  $\delta$  Sct stars in the LMC from the OGLE-III project was published by Poleski *et al.* (2010a). Stars of this type usually have magnitudes which are at the observing limits of the OGLE project photometry, so for most of them our classification is rather uncertain. In the GSEP region we detected 159  $\delta$  Sct stars. Among them 10 objects show double-mode behavior, with the period ratios between 0.76 and 0.79 – typical for fundamental-mode/first-overtone pulsators (Pigulski *et al.* 2006). Two  $\delta$  Sct stars oscillate in the first and second overtones. Fig. 9 shows newly found double-mode  $\delta$  Sct stars in the Petersen diagram, together with variables from the catalog of Poleski *et al.* (2010a).

#### *Long Period Variables*

Long-period variables (LPVs) constitute the most numerous group of variable stars in the GSEP Field Catalog. In total we identified 2819 LPVs in the four OGLE-IV fields. As in the OGLE-III catalog of LPVs in the Magellanic Clouds



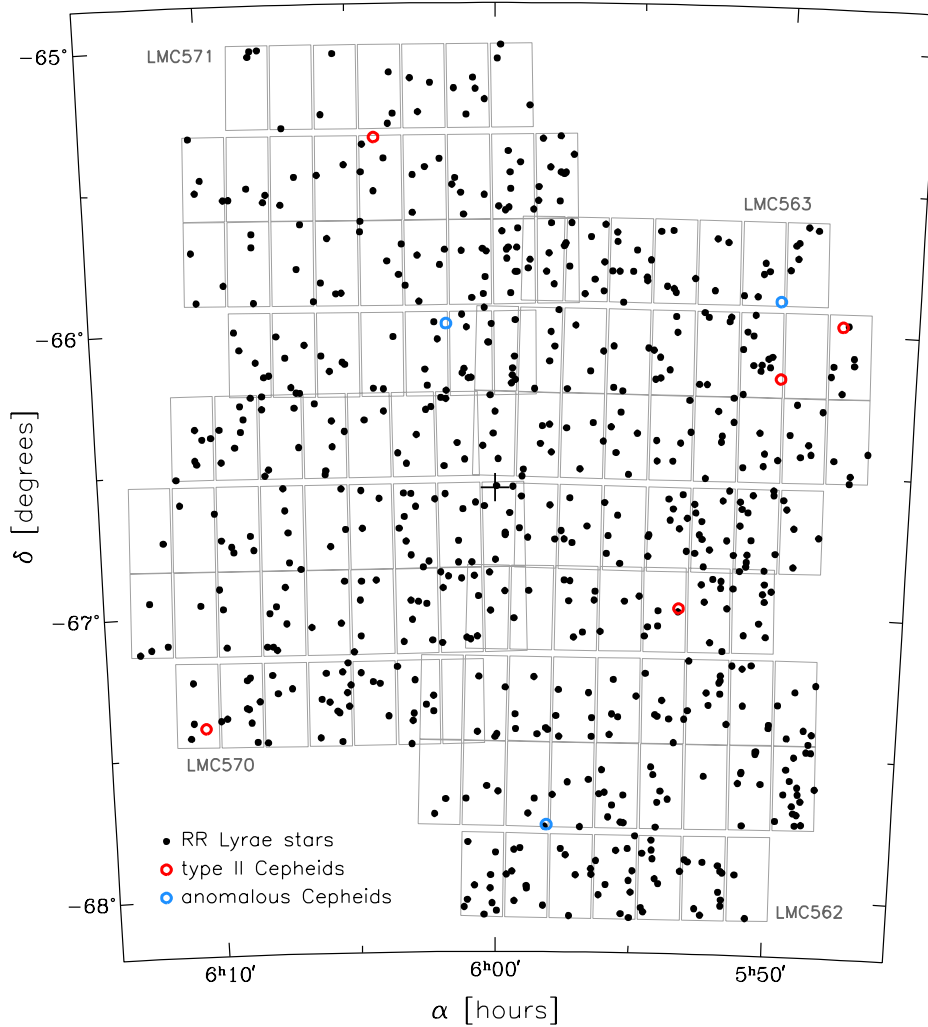


Fig. 11. Spatial distribution of RR Lyr stars, type II Cepheids and anomalous Cepheids in the GSEP field. Gray contours show the sky coverage by the individual chips of the OGLE-IV mosaic CCD camera. Black, red and blue symbols show positions of RR Lyr stars, type II Cepheids and anomalous Cepheid, respectively. Black cross indicates the position of the South Ecliptic Pole.

(Soszyński *et al.* 2009b), we divided our sample of pulsating red giants into three groups: Miras, semiregular variables (SRVs) and OGLE small amplitude red giants (OSARGs). We used the same criteria of our classification, *i.e.*, as Miras we recognized stars with the peak-to-peak amplitude of the detrended *I*-band light curve larger than 0.8 mag, while OSARGs differ from SRVs by their separate period–luminosity relations (in the *K*-band and Wesenheit indices) and characteristic period ratios (Soszyński *et al.* 2007). Note that in this work we applied these criteria to the light curves spanning only two years, and in the future, with more data and longer time span, our classification of some individual objects may change.

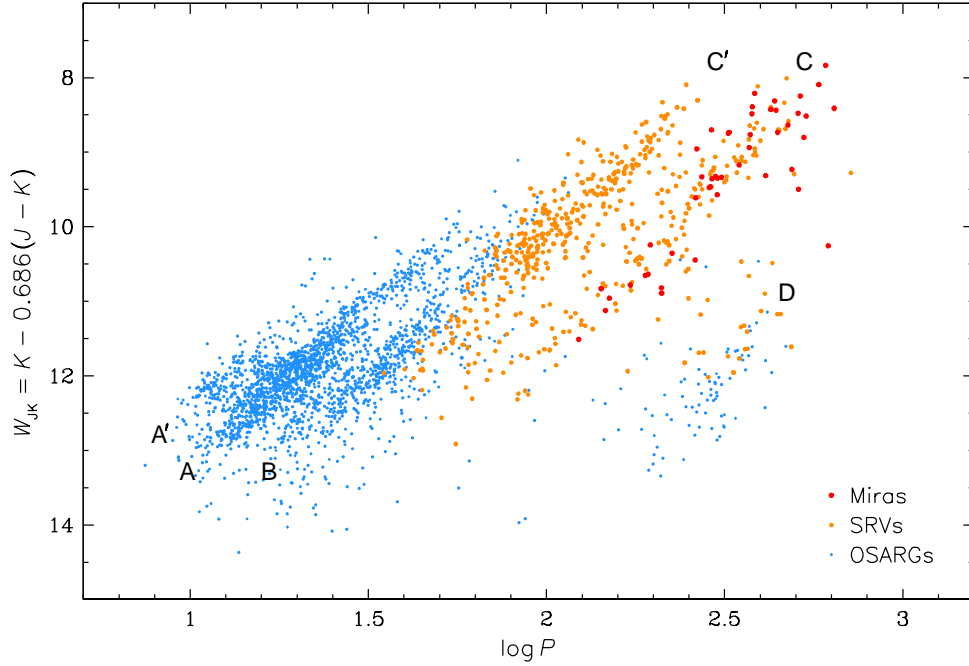


Fig. 12. Near-infrared Wesenheit index vs. luminosity diagram for long-period variables in the GSEP field. Blue, orange and red points indicate OSARGs, SRVs and Mira stars. Labels show the PL sequences introduced by Wood *et al.* (1999). Each star is represented by one, the primary period. Near-infrared measurements were taken from the 2MASS catalog (Cutri *et al.* 2003).

The near-infrared period–luminosity diagram (as a “luminosity” we used the reddening-free Wesenheit index, defined as  $W_{JK} = K - 0.686(J - K)$ ) for LPVs (Fig. 12) reveals the well known pattern, noticed for the first time by Wood *et al.* (1999). The only small difference can be seen for the longest-period giants, in particular in sequence D populated by stars with the so called long-secondary periods. This is due to relatively short time baseline of our observations.

#### *Eclipsing and Ellipsoidal Binaries*

Our search for variable stars resulted in the detection of 1533 binary systems, usually eclipsing or ellipsoidal variables. All of them are new findings. The Galactic star LMC570.22.45 shows the shortest orbital period of 3.361 hours. The longest-period binaries are ellipsoidal red giants, with periods reaching several hundred days. The distributions of colors and magnitudes of our binary systems are similar to the distributions of the whole population of stars in the OGLE database, which means that faint objects dominate in the list of eclipsing binaries. Since the light curves of faint stars are usually noisy, we have not divided our sample into contact, semi-detached and detached systems.

Our catalog contains several interesting cases. LMC562.11.9469 shows overlapping ellipsoidal and eclipsing light curves, with the orbital periods of 421.5 days

and 1.712147 days, respectively. At least ten eclipsing binaries exhibit additional variations with periods close (but not equal) to the orbital periods – the feature typical for RS CVn variable stars. We flagged these objects in the catalog remarks. Four eclipsing variable stars show additional periods from 29 to 40 times longer than their orbital periods. These objects belong to the so called double-periodic variables (DPVs) – a class of binaries discovered by Mennickent *et al.* (2003) in the OGLE data. Poleski (2010b) published the catalog of 125 DPVs in the LMC.

#### *Other Variable Stars*

Our catalog also contains 1473 periodic and non-periodic objects classified as OTHER variable stars. Their variability type cannot be unambiguously determined from the available data or the classification is uncertain. Many of these objects show characteristic features of the rotating spotted stars. This group likely contains also binary systems, Be stars,  $\delta$  Sct and other pulsating stars. Additional information like spectral features could be conclusive in these cases for proper interpretation.

## **5. OGLE-IV Support for Gaia Science Alerts System**

The data processing pipeline of Gaia is designed for near-real-time alerting on detections of anomalies or brightenings or appearances of new objects. The alerting system will be operating already during the commissioning phase of Gaia, but will be thoroughly tested on these first scientific Gaia data. The pipeline will exploit both photometry and low-resolution spectroscopy to identify potential transient events (Wyrzykowski and Hodgkin 2012).

As the OGLE-IV GSEP field can be the first testing point for the Gaia Alert system, we took a closer look at the transients that can be detected and expected in this region of the sky. We also prepared ground based data facilitating the detection and interpretation of potential supernovae by Gaia.

### *5.1. Search for OGLE-IV Transient Objects in the GSEP Field*

Apart from searching for ordinary variable stars, we conducted independent search of the OGLE-IV databases for transient events. We searched both the main OGLE-IV databases and the databases of new objects. The latter contain objects that are not present on the DIA reference images, so they seem to appear from below the detection threshold level. In such sparse stellar density fields, we expect to find several supernovae (SNe) exploding in background galaxies. There are eleven such findings. Two of them are most likely SN Ia and the remaining nine are also good SN candidates.

The supernova OGLE-2011-SN-003 (Fig. 13) appeared  $2.''7$  away from a nearly edge-on galaxy OGLE-GALAXY-LMC563.17.14 (see Section 5.2 describing the galaxy catalog). The second object – supernova OGLE-2011-SN-004, (Fig. 14) was

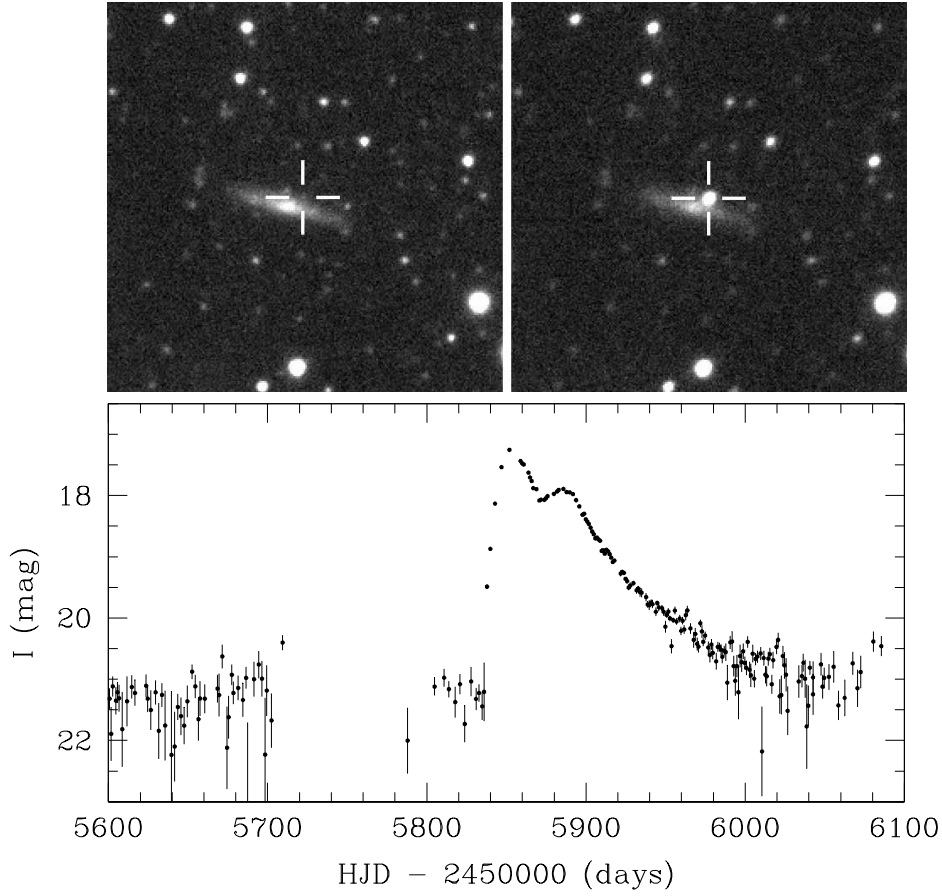


Fig. 13. *Top*: Finding chart for supernova OGLE-2011-SN-003. *Left image* shows the galaxy before SN explosion, while the *right image* shows the SN at its peak (marked with cross hairs). It is located  $2''.7$  away from a nearly edge-on galaxy OGLE-GALAXY-LMC563.17.14. The image covers  $60'' \times 60''$ . *Bottom*: OGLE-IV light curve for SN OGLE-2011-SN-003. It peaked at  $I = 17.27$  mag on 2011, October 17. The gap at  $5700 < \text{HJD} - 2450000 < 5800$  is the seasonal gap, when the LMC is not observable.

detected  $10''.7$  away from an elliptical galaxy OGLE-GALAXY-LMC570.28.8. Both these objects were found during the search of the databases of new objects. An artificial blend star of  $I = 20.65$  mag was added to the light of both objects to avoid undefined magnitudes when the stars were not detectable on the frames before and after brightening.

The additional nine objects were found during the search of regular OGLE-IV databases. Faint galaxies often mimic faint stars and therefore they are included to these databases. Explosion of a SN in such a galaxy can be recognized by a characteristic spike on the otherwise flat and noisy galaxy light curve. Additional visual confirmation on the reference image that the object is indeed a galaxy makes the SN interpretation of a transient very sound.

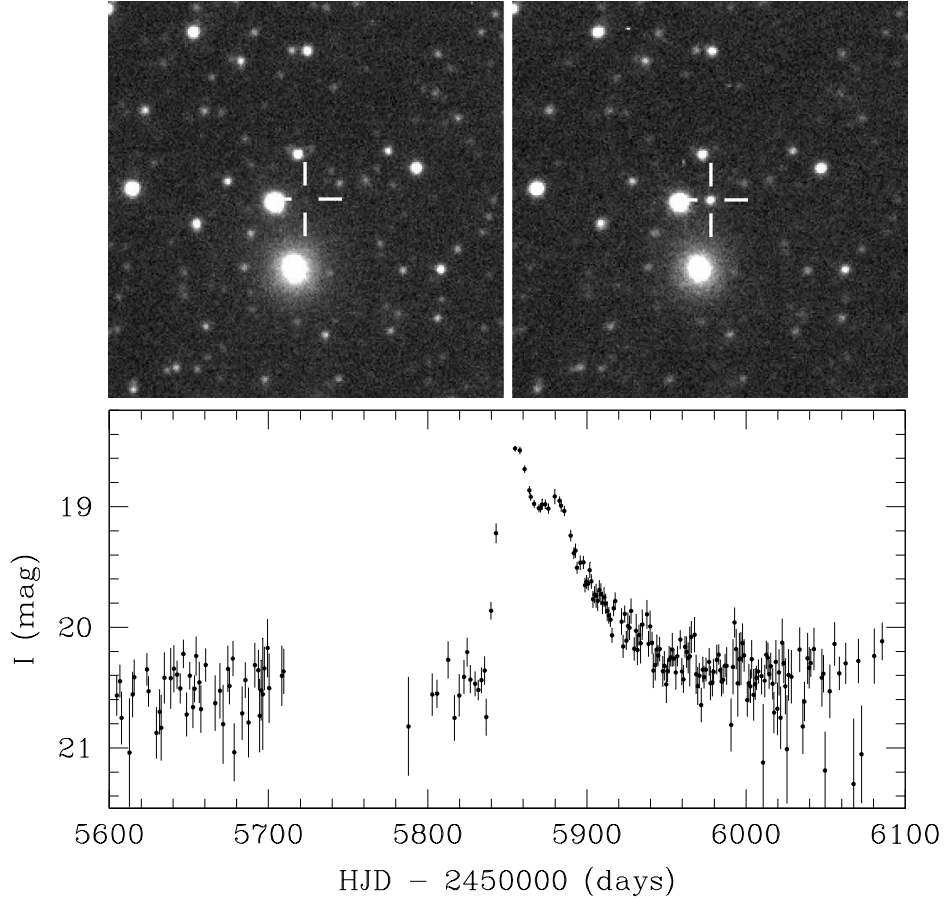


Fig. 14. *Top*: Finding chart for supernova OGLE-2011-SN-004. *Left image* shows the galaxy before SN explosion, while the *right image* shows the SN at its peak (marked with cross hairs). It is located  $10''.7$  away from an elliptical galaxy OGLE-GALAXY-LMC570.28.8. The image covers  $60'' \times 60''$ . *Bottom*: OGLE-IV light curve for SN OGLE-2011-SN-004. It peaked at  $I = 18.51$  mag on 2011, October 20.

An example of an interesting SN candidate found in this search, OGLE-2011-SN-001, is presented in Fig. 15. The light curve clearly shows a supernova-type spike superimposed on the long term brightening. Next observing season, after the fading of the main supernova-like peak – the second brightening episode clearly occurred. Evidently, this object is located on the faint galaxy, therefore it is likely a supernova candidate.

Table 3 lists all the SN candidates detected in the OGLE-IV GSEP field. Their light curves are available in the OGLE Internet archive (see Section 7).

The detection of eleven SNe candidates in the GSEP field over 2.2 years indicates the rate of SN occurrence of about 2 SN per year per square degree including the seasonal gaps (20% of time) in observations and assuming about 70–80% detection efficiency. This is a similar rate to that found during the search for SNe in

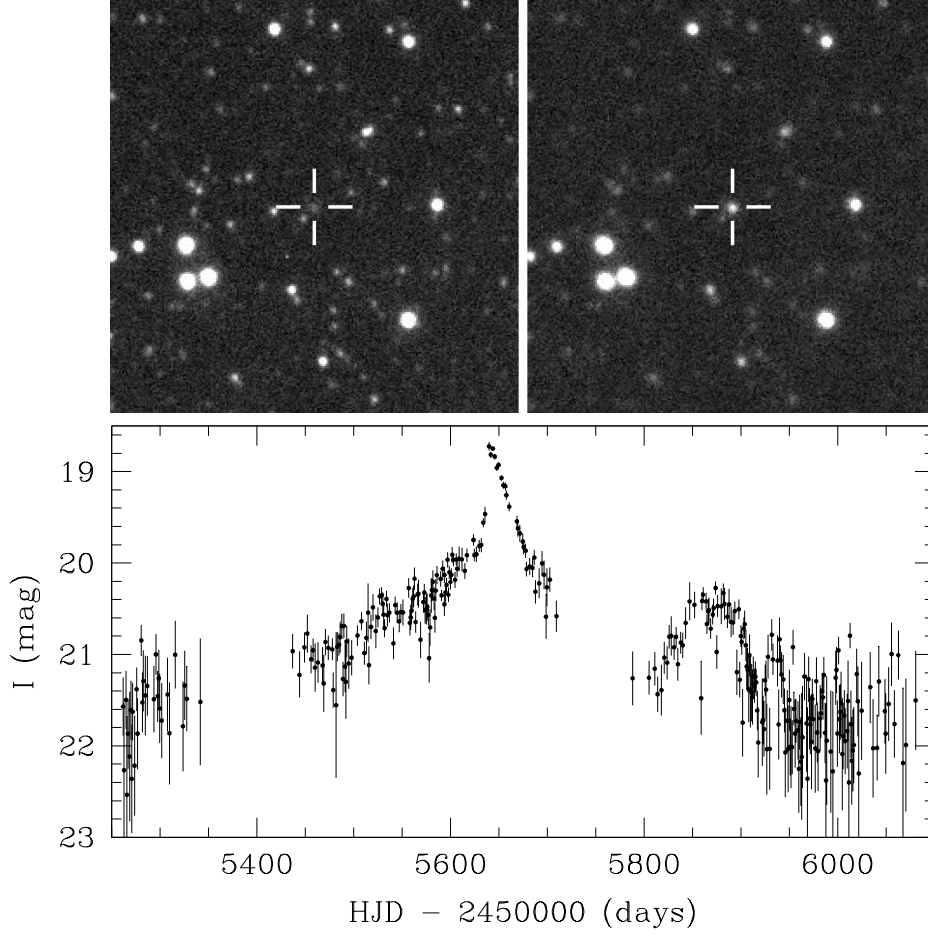


Fig. 15. *Top*: Finding chart for supernova candidate, OGLE-2011-SN-001. *Left image* shows the galaxy before SN explosion, while the *right image* shows the SN at its peak (marked with cross hairs). *Bottom*: OGLE-IV light curve for SN candidate OGLE-2011-SN-001. It peaked at  $I = 18.74$  mag on 2011, March 19.

the neighboring Magellanic Bridge fields also observed by OGLE-IV for similar period of time (Kozłowski *et al.* 2012, in preparation).

### 5.2. Catalog of Galaxies

Identification and confirmation of supernovae, one of the main targets of the Gaia alerting pipeline, will benefit strongly if the possible supernova was cross-matched with a nearby galaxy. OGLE-IV images of the GSEP region provide an excellent material for cataloging most of the galaxies up to redshift  $z \approx 0.1$ , which is the expected limit for supernovae to be detected by Gaia.

We searched for galaxies in the OGLE-IV GSEP field images using SEXTRACTOR (Bertin and Arnouts 1996) running on the DIA reference  $I$ -band images. We selected as potential galaxies all objects brighter than 17.5 mag with

Table 3  
SN candidates in the GSEP Field

ID	OGLE-IV Object ID	R.A. [2000.0]	Dec [2000.0]	$I_{\max}$ [mag]	$T_{\max}$ JD [days]	Remarks
OGLE-2010-SN-001	LMC571.04.7642	06 <sup>h</sup> 04 <sup>m</sup> 14 <sup>s</sup> 54	−66°00′24″3	19.73	2 455 545	G1
OGLE-2011-SN-001	LMC563.10.12139	05 <sup>h</sup> 57 <sup>m</sup> 27 <sup>s</sup> 81	−66°21′42″6	18.74	2 455 640	G
OGLE-2011-SN-002	LMC571.23.5674	06 <sup>h</sup> 01 <sup>m</sup> 00 <sup>s</sup> 48	−65°25′51″9	20.15	2 455 813	G2
OGLE-2011-SN-003	LMC563.17.499N	05 <sup>h</sup> 59 <sup>m</sup> 50 <sup>s</sup> 14	−65°56′22″8	17.27	2 455 852	G3
OGLE-2011-SN-004	LMC570.28.179N	06 <sup>h</sup> 07 <sup>m</sup> 16 <sup>s</sup> 62	−66°20′24″0	18.51	2 455 855	G4
OGLE-2011-SN-005	LMC571.28.4728	06 <sup>h</sup> 05 <sup>m</sup> 24 <sup>s</sup> 89	−65°03′03″1	19.79	2 455 858	G5
OGLE-2011-SN-006	LMC570.31.2207	06 <sup>h</sup> 02 <sup>m</sup> 12 <sup>s</sup> 93	−66°27′45″8	19.83	2 455 913	
OGLE-2012-SN-001	LMC563.32.5268	05 <sup>h</sup> 49 <sup>m</sup> 45 <sup>s</sup> 04	−65°47′46″9	19.73	2 455 940	G
OGLE-2012-SN-002	LMC571.04.3566	06 <sup>h</sup> 04 <sup>m</sup> 34 <sup>s</sup> 87	−66°06′13″6	19.59	2 455 956	G
OGLE-2012-SN-003	LMC570.12.8488	06 <sup>h</sup> 06 <sup>m</sup> 30 <sup>s</sup> 17	−66°57′04″2	19.53	2 455 992	G
OGLE-2012-SN-004	LMC571.19.642	06 <sup>h</sup> 06 <sup>m</sup> 44 <sup>s</sup> 62	−65°35′49″4	19.43	2 456 007	G

Notes: G – SN host galaxy is present on the template image,  
G1 – galaxy OGLE-GALAXY-LMC571.04.11,  
G2 – galaxy OGLE-GALAXY-LMC571.23.12,  
G3 – galaxy OGLE-GALAXY-LMC563.17.14,  
G4 – galaxy OGLE-GALAXY-LMC570.28.8,  
G5 – galaxy OGLE-GALAXY-LMC571.28.22.

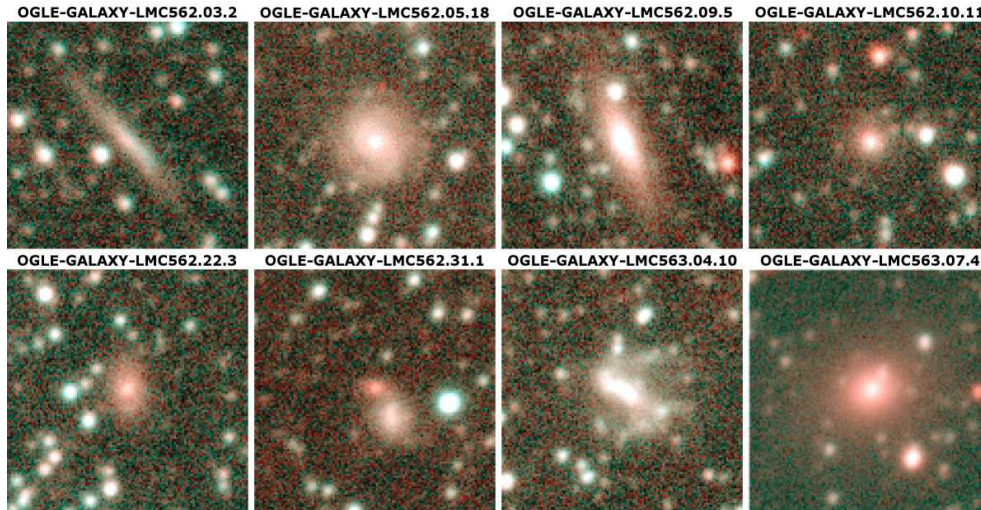


Fig. 16. Examples of galaxies identified in the OGLE-IV reference images of the GSEP field.

class\_star < 0.15 and brighter than 18.7 mag with class\_star < 0.01. Then, we visually inspected all of about 4000 candidates to select 1925 apparent galaxies. Fig. 16 shows examples of identified galaxies as a false-color composition of  $I$ - and  $V$ -band images. Fig. 17 shows the locations of all identified galaxies on the map of OGLE-IV GSEP field, with red and blue points representing galaxies brighter and fainter, respectively, than 18 mag in the  $I$ -band. Table containing all 1925 candidate

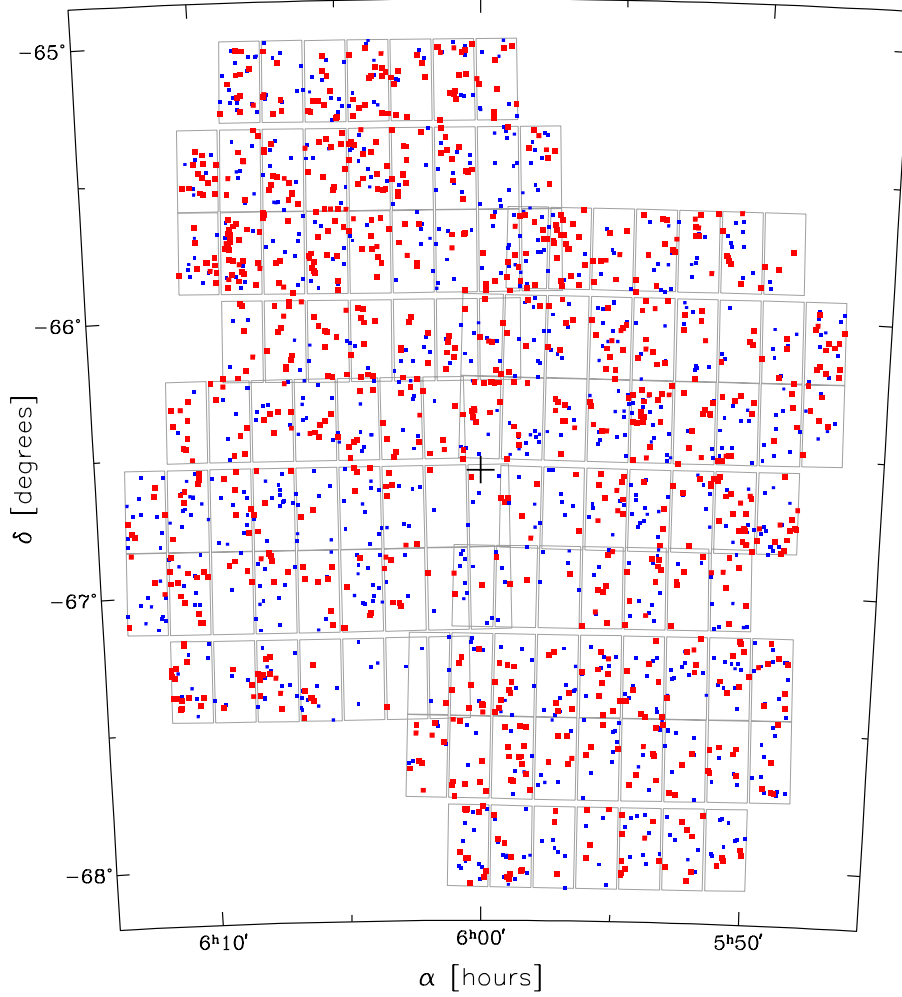


Fig. 17. Spatial distribution of galaxies detected in the GSEP field. Gray contours show the sky coverage by the individual chips of the OGLE-IV mosaic CCD camera. Red and blue symbols show positions of galaxies brighter and fainter, respectively, than 18 mag in the  $I$ -band. Black cross indicates the position of the South Ecliptic Pole.

galaxies, along with their coordinates and  $I$ -band magnitudes is available from the OGLE Internet archive (see Section 7).

## 6. Astrometry of the GSEP Field

The OGLE images collected at one of the best observational sites worldwide, Las Campanas Observatory, with high angular resolution of the OGLE cameras and long time span are ideal observational material for astrometric purposes (Poleski *et al.* 2012). Therefore, we additionally analyzed the time-series astrometry of all stars brighter than  $I = 19.5$  mag in the GSEP field. The centroids of the stellar im-



ages were measured for each epoch separately using our own code which is based on method presented by Anderson and King (2000). The proper motions and parallaxes were derived similarly to Poleski *et al.* (2012) and are tied to the LMC stars. The typical accuracy of the derived proper motions is 1.8 mas/yr per coordinate, while typical accuracy of the parallaxes is 1.5 mas. We failed in analyzing two subfields namely LMC570.17 and LMC571.17.

In total, we derived reliable proper motions for 3309 stars from the GSEP field. To avoid artifacts we only selected objects with  $\chi^2$  of the astrometric fit smaller than 2.5, positive cross-match in at least 70% of well registered epochs of the given subfield and proper motion greater than 20 mas/yr. The stars with proper motions greater than 50 mas/yr were visually verified. For the stars with proper motions between 20 mas/yr and 50 mas/yr the false positive rate is 10% and the list is complete in 90%.

Significant proper motions were measured for 50 variable stars, which clearly indicates that these stars belong to the Milky Way. We also found 50 non-variable high proper motion (HPM) stars, *i.e.*, the ones with the proper motion larger than 100 mas/yr or slightly below that limit, but with parallaxes greater than 10 mas. Based on measured parallaxes, *I*-band magnitudes and  $(V - I)$  colors we found three of the HPM stars to be nearby white dwarfs.

The file pm.dat in the OGLE Internet archive lists all objects with reliable astrometry found in the GSEP field. For each star, apart from the OGLE-IV identification number, coordinates and mean brightness in the *I*- and *V*-bands, we present the proper motion in right ascension and declination with uncertainties.

Additionally, the file hpm.dat contains the results of our search for HPM stars. Here, in addition to the information provided in pm.dat file the equatorial coordinates of the object position at the J2000 epoch are given. Please note that the position of some of the stars listed in this file changed up to 4'' on OGLE-IV images taken more than ten years after the J2000 epoch. Also, for all objects the parallax and its uncertainty are given. Three white dwarfs found are marked.

One has to remember that the OGLE-IV astrometry is based on relatively short time baseline of only 26 months. The data presented here will be superseded in the future by the next releases of the OGLE astrometric catalogs.

## 7. Data Availability

All data presented in this paper are available to the astronomical community from the OGLE Internet archive accessible from the OGLE WWW Page or directly:

<http://ogle.astrouw.edu.pl>  
<ftp://ftp.astrouw.edu.pl/ogle/ogle4/GSEP>

Please read the README file for the details on the data presented there as well as on all updates.

**Acknowledgements.** We would like to thank Z. Kołaczowski and A. Schwarzenberg-Czerny for providing software which enabled us to prepare this study. We would also like to thank G. Clementini and L. Eyer for stimulating discussions about this project.

The OGLE project has received funding from the European Research Council under the European Community's Seventh Framework Programme (FP7/2007-2013)/ERC grant agreement no. 246678 to AU. This work has been supported by the Polish National Science Centre grant no. DEC-2011/03/B/ST9/02573. The astrometric part of the research was supported by Polish Ministry of Science and Higher Education through the program "Iuventus Plus" award No. IP2011 043571 to RP.

## REFERENCES

- Alard, C., and Lupton, R.H. 1998, *ApJ*, **503**, 325.
- Anderson, J., and King, I.R. 2000, *PASP*, **112**, 1360.
- Artyukhina, N.M., *et al.* 1995, General Catalogue of Variable Stars, 4rd ed., vol.V. Extragalactic Variable Stars, "Kosmosinform", Moscow.
- Bertin, E., and Arnouts, S. 1996, *A&AS*, **117**, 393.
- Cioni, M.-R.L., Clementini, G., Girardi, L., *et al.* 2011, *A&A*, **527**, A116.
- Cutri, R.M., *et al.* 2003, "2MASS All-Sky Catalog of Point Sources".
- de Bruijne, J.H.J. 2012, *Ap&SS*, **341**, 31.
- Leavitt, H.S. 1908, *Ann. Harv. Coll. Obs.*, **60**, 87.
- Mennickent, R.E., Pietrzyński, G., Diaz, M., and Gieren, W. 2003, *A&A*, **399**, L47.
- Pietrzyński, G., Thompson, I.B., Gieren, W., Graczyk, D., Bono, G., Udalski, A., Soszyński, I., Minniti, D., and Pilecki, B. 2010, *Nature*, **468**, 542.
- Pietrzyński, G., Thompson, I.B., Graczyk, D., Gieren, W., Pilecki, B., Udalski, A., Soszyński, I., Bono, G., Konorski, P., Nardetto, N., and Storm, J. 2011, *ApJ*, **742**, L20.
- Pigulski, A., Kołaczowski, Z., Ramza, T., and Narwid, A. 2006, *Mem. Soc. Astron. Ital.*, **77**, 223.
- Pojmański, G. 1997, *Acta Astron.*, **47**, 467.
- Poleski, R., Soszyński, I., Udalski, A., Szymański, M.K., Kubiak, M., Pietrzyński, G., Wyrzykowski, Ł., Szewczyk, O., and Ulaczyk, K. 2010a, *Acta Astron.*, **60**, 1.
- Poleski, R., Soszyński, I., Udalski, A., Szymański, M.K., Kubiak, M., Pietrzyński, G., Wyrzykowski, Ł., and Ulaczyk, K. 2010b, *Acta Astron.*, **60**, 179.
- Poleski, R., Soszyński, I., Udalski, A., Szymański, M.K., Kubiak, M., Pietrzyński, G., Wyrzykowski, Ł., and Ulaczyk, K. 2012, *Acta Astron.*, **62**, 1.
- Schwarzenberg-Czerny, A. 1996, *ApJ*, **460**, L107.
- Shapley, H., and Mohr, J. 1933, *Ann. Harv. Col. Obs.*, **90**, 1.
- Soszyński, I., Dziembowski, W.A., Udalski, A., Kubiak, M., Szymański, M.K., Pietrzyński, G., Wyrzykowski, Ł., Szewczyk, O., and Ulaczyk, K. 2007, *Acta Astron.*, **57**, 201.
- Soszyński, I., Poleski, R., Udalski, A., Szymański, M.K., Kubiak, M., Pietrzyński, G., Wyrzykowski, Ł., Szewczyk, O., and Ulaczyk, K. 2008, *Acta Astron.*, **58**, 163.
- Soszyński, I., Udalski, A., Szymański, M.K., Kubiak, M., Pietrzyński, G., Wyrzykowski, Ł., Szewczyk, O., Ulaczyk, K., and Poleski, R. 2009a, *Acta Astron.*, **59**, 1.
- Soszyński, I., Udalski, A., Szymański, M.K., Kubiak, M., Pietrzyński, G., Wyrzykowski, Ł., Szewczyk, O., Ulaczyk, K., and Poleski, R. 2009b, *Acta Astron.*, **59**, 239.
- Szymański, M.K., Udalski, A., Soszyński, I., Kubiak, M., Pietrzyński, G., Poleski, R., Wyrzykowski, Ł., and Ulaczyk, K. 2011, *Acta Astron.*, **61**, 83.
- Tisserand, P., Le Guillou, L., Afonso, C., *et al.* 2007, *A&A*, **469**, 387.

- Udalski, A. 2003, *Acta Astron.*, **53**, 291.
- Udalski, A., Szymański, M.K., Soszyński, and Poleski, R. 2008, *Acta Astron.*, **58**, 69.
- Wetzel, M.A. 1955, *Ann. Harv. Col. Obs.*, **109**, 58.
- Wood, P.R., *et al.* (MACHO team) 1999, in: *IAU Symp.* 191, “Asymptotic Giant Branch Stars”, ed. T. Le Bertre, A. Lébre, and C. Waelkens (San Francisco: ASP), p. 151.
- Woźniak, P.R. 2000, *Acta Astron.*, **50**, 421.
- Wyrzykowski, Ł., and Hodgkin, S. 2012, in *IAU Symp.* 285, New Horizons in Time-Domain Astronomy, ed. R. E. M. Griffin, R. J. Hanisch, and R. Seaman (Cambridge: Cambridge Univ. Press), 425.